JOURNAL OF GEOPHYSICAL RESEARCH, VOL. 105, NO. C4, PAGES 8549–8564, APRIL 15, 2000

Spreading of Red Sea overflow waters in the Indian Ocean

Lisa M. Beal,[1] Amy Ffield, and Arnold L. Gordon

Lamont-Doherty Earth Observatory of Columbia University, Palisades, New York

Abstract. As a result of its remarkably high salinity and despite its small volume input, remnants of Red Sea Water (RSW) have been identified in the Agulhas Current, over 6000 km distant of their source. This provided the motivation to investigate the long-term mean spreading of RSW throughout the Indian Ocean, using a comprehensive set of observations, taken from the National Oceanographic Data Center archives and from the World Ocean Circulation Experiment Hydrographic Program for the Indian Ocean. After emerging from the Gulf of Aden into the Arabian Sea, RSW spreads predominantly southwestward along the African continental slope, as indicated by strongly inclined isohalines across the Arabian Sea. There is some monsoon variability, so that during the winter monsoon there is more RSW present in the Gulf of Aden and an intensification of southward spreading along the western boundary, between 12° and 5°N. Elsewhere the intermediate depth salinity field of the Indian Ocean appears relatively stationary. Between 5° and 10°S, in the region of the South Equatorial Current, isohalines of the RSW layer become quasi-zonal across the width of the Indian Ocean, only dipping southward toward the western boundary west of 50°E. South of here, there is a strong tongue of RSW spreading southward through the Mozambique Channel and into the Agulhas Current. These conclusions concur with previous localized investigations of intermediate water properties. Using a simple mixing model, the percentage of RSW throughout the Indian Ocean was quantified. It was found that the flux of salt into the Gulf of Aden from the Red Sea is similar to that estimated to cross 32°S in the Agulhas Current. This result implies that all the RSW which is mixed into the interior of the Indian Ocean may eventually be exported at the western boundary. Furthermore, it implies that RSW is the dominant component of the salt budget for the intermediate layer and that input from the Indonesian Seas and via diapycnic processes are small.

1. Introduction

The volume transport of Red Sea overflow waters is very small, yet observations taken throughout the Indian Ocean during the World Ocean Circulation Experiment (WOCE) Hydrographic Program (WHP) and before show Red Sea Water (RSW) to have a distinctive and far reaching signal. Despite an annual mean of just 0.37 Sv (Sv = 1×10^6 m^3 s^{-1}) flowing from the Red Sea through the Bab el Mandeb strait [*Murray and Johns*, 1997], intermediate depth, high salinities of Red Sea origin are consistently found in the southwest Indian Ocean, thousands of kilometers from the strait. For example, the influence of RSW has been measured in the Agulhas Current at 32°S on each of four occasions: during *Darwin's* transindian section in November 1987 [*Toole and Warren*, 1993], during *Discovery* WHP cruise ICM1 in February 1995 [*Beal and Bryden*, 1997], during the *Baldridge* WHP cruise of March 1995, and during the *Knorr* WHP cruise I5W in June 1995. Remnants of RSW have also been observed in the Agulhas retroflection region to the south of South Africa [*Gordon et al.*, 1987; *Valentine et al.*, 1993]. The presence of a RSW signature some 6000 km from its source results from the extreme high salinity of the Red Sea outflow, which survives as a strong intermediate salinity maximum after diapycnal mixing and dilution in the Gulf of Aden. This salinity signal is compounded at intermediate depths by an extreme oxygen minimum, which has its source in the northern Arabian Sea [*Olson et al.*, 1993]. In addition, the salinity maximum of RSW is in sharp contrast to the salinity minimum of Antarctic Intermediate Water (AAIW), which spreads into the Indian Ocean from the south at a similar density interval.

[1]Now at Scripps Institution of Oceanography, La Jolla, California.

Copyright 2000 by the American Geophysical Union.

Paper number 1999JC900306.
0148-0227/00/1999JC900306$09.00

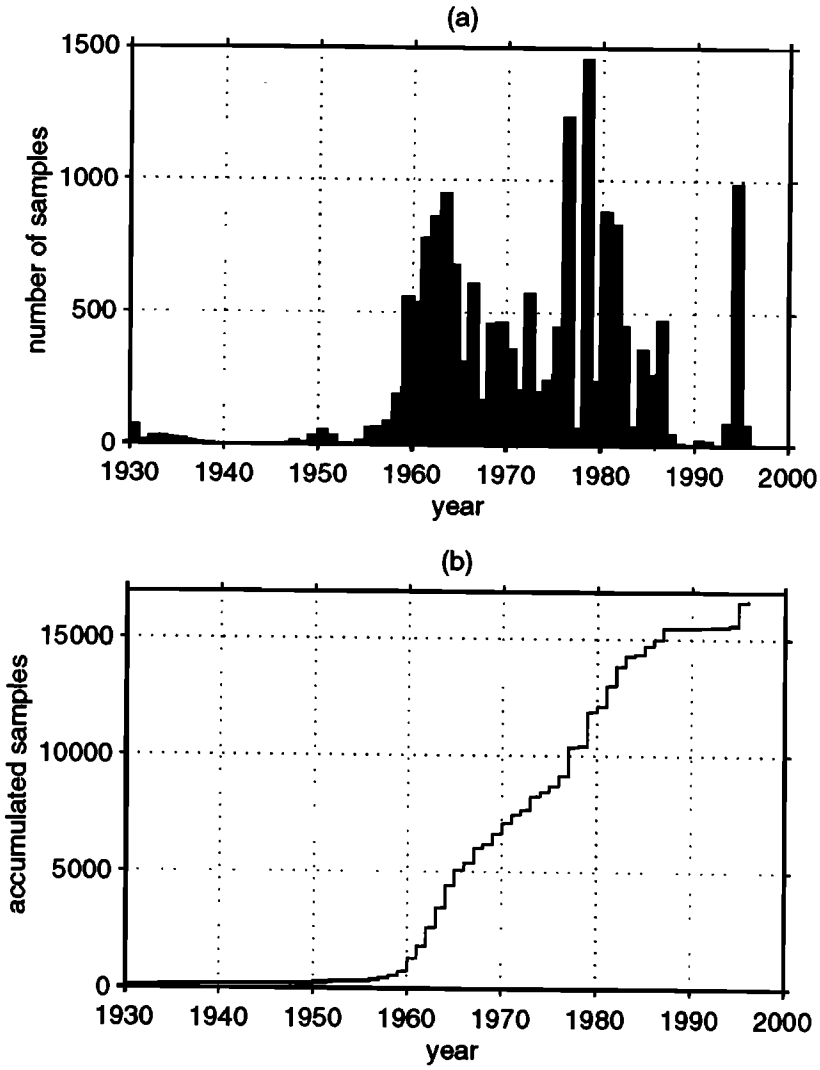

Figure 1. Number of salinity station data available in the Indian Ocean between densities $\sigma_1 = 31.5$ and 32.1 ($\sigma_0 = 27.0$ and 27.6) in the combined National Oceanographic Data Center (NODC) and World Ocean Circulation Experiment (WOCE) databases.

Consequently, RSW and the Arabian Sea low-oxygen layer are remarkable tracers for the mid-depth circulation throughout much of the Indian Ocean.

Since *Wyrtki* [1971] mapped the large-scale spreading pattern of RSW within the Indian Ocean, the temperature and salinity data available for such an analysis have more than doubled, from around 7,000 to 17,000 stations (Figure 1). More recently, *You and Tomczak* [1993] addressed the circulation of thermocline waters in the Indian Ocean and included RSW in their analysis, producing maps down to the $\sigma_0 = 27.3$ density surface. However, this surface occurs at approximately the midpoint of the thickness of RSW influence [*Warren et al.*, 1966] and therefore is unable to fully resolve the layer. Furthermore, in their source water type definitions, *You and Tomczak* [1993, Table 1] define RSW as a saline water on $\sigma_0 = 25.7$. These waters occur at depths shallower than 200 m, and in fact, their source is not in the Red Sea, but in the northern Arabian Sea, as indicated by You and Tomczak's own Figure 8b, by *Wyrtki* [1971], and by *Bower et al.* [1999]. At $\sigma_0 = 27.3$, the core density of RSW [*Wyrtki*, 1971], *You and Tomczak* [1993] discount the contribution of RSW all together. Hence we see a need for a more specific analysis, using contemporary data sets, to better describe the circulation of the RSW layer.

An annual mean volume of 0.37 Sv of RSW overflows into the Gulf of Aden through the Bab el Mandeb Strait with salinities over 40 [*Murray and Johns*, 1997]. As the overflow descends along topography and entrains many times its own volume of Gulf water, its properties change dramatically. *Bower et al.* [1999] use a combination of observations and a model to show that, on the average, the overflow reaches neutral bouyancy within 40 km of the strait, equilibrating with salinity 37.5 and temperature 18.1°C at $\sigma_0 = 27.2$ ($\sigma_1 \approx 31.7$). There is much evidence of inhomogeniety to this layer, with extensive interleaving of

relatively fresh waters within the RSW. In fact, interleaving appears to be a characteristic of RSW influence wherever it is found in the Indian Ocean; for example, *Fedorov and Meschanov* [1988] observed interleaving in the Arabian Sea, *Gründlingh* [1985] observed it in the Mozambique Channel and *Beal* [1997] found interleaving in the Agulhas Current. Perhaps the high-salinity contrasts make double-diffusive processes more visible. Once outside the Gulf of Aden, RSW has been observed in lenses principally in the western Arabian Sea but also toward its center during the southwest monsoon [*Gamsakhurdiya et al.*, 1991]. In the Somali Basin, *Warren et al.* [1966] note the influence of RSW between $\sigma_0 = 27.0$ and 27.6, and *Quadfasel and Schott* [1982] find that RSW crosses the equator close to the western boundary at depths of about 750 m. *Wyrtki* [1971] used the intermediate depth salinity maximum to show that south of the equator there is a tongue of RSW which enters the Mozambique Channel; however, this maximum was traced no farther south than 23°S, owing to the northward spreading of low-salinity AAIW from the Southern Ocean. *Gründlingh* [1985] observed lenses of very high salinity waters above the Mozambique Ridge at 28°S. *Toole and Warren* [1993] observed a filament of RSW with a core salinity of 34.65 on $\sigma_0 = 27.6$, over the continental slope within the Agulhas Current at 32°S, and both *Gordon et al.* [1987] and *Valentine et al.* [1993] report occurrences of RSW farther south in the Agulhas retroflection region.

Here we examine the spreading of RSW from its product waters in the Gulf of Aden to its export at the southern extent of the Indian Ocean, tracing the water mass within an isopycnic layer. Historical data together with the preliminary results from the WHP are used in the analysis. The possible effect of the monsoons on the spreading of RSW is also investigated. A salt budget for the intermediate layer is estimated in order to determine the importance of the input of salt from the Red Sea, and a simple water mass mixing model is used to quantify the amount of RSW present in different regions of the Indian Ocean. Finally, the layer potential vorticity field is calculated to help illustrate preferred pathways of RSW spreading.

2. Data and Methods

The data set is a comprehensive combination of National Oceanographic Data Center (NODC) archived Conductivity-Temperature-Depth (CTD) and bottle measurements (updated as of March 1998) within 20° to 120°E and 30°N to 40°S plus the WHP Indian Ocean preliminary data set. The NODC archive includes measurements taken since the 1920s; however, all but 200 or so of the 17,000 stations used here for the mapping of the "RSW layer" (see section 3 for a definition of this layer) were collected after the second world war (Figure 1). Nominally then, the data set covers some 50 years. The number of samples shown in Figure 1 corresponds to those stations where data are available to a density of at least $\sigma_1 = 32.1$ ($\sigma_0 \approx 27.6$) or as deep as 1600 dbar in the southwest Indian Ocean. At shallower depths the number of stations increases rapidly; for example, in the core of the RSW influence on $\sigma_1 = 31.8$ ($\sigma_0 \approx 27.3$), at depths from 800 to 1200 dbar [*Wyrkti*, 1971], there are 24,683 stations. The positions of these stations are shown in Plate 1. Data are color-coded for salinity intervals of 0.1 from 34.3 to 35.6; salinities greater than 35.6 are shown in dark red and reach over 40 in the Red Sea. Obvious outliers were eliminated manually from the data, not by using an algorithm. This is because the nature of RSW is such that it often appears as a relatively isolated salinity anomaly, and therefore removing anomalies automatically would remove much of our signal. For example, *Rochford* [1966] and *Warren et al.* [1966] have shown that locally in the northwest Indian Ocean the horizontal gradient of intermediate salinity can be greater than the large-scale gradients over the whole of the western Indian Ocean, and *Beal and Bryden* [1999] find a transition in salinity from 34.46 to 34.65 (AAIW to RSW) over a distance of just 60 km in the intermediate waters of the Agulhas Current in the southwest Indian Ocean.

Our analysis is carried out on isopycnal surfaces because isobaric smoothing distorts water mass properties [*Lozier et. al*, 1994]. Potential density was calculated relative to 1000 dbar. Properties along individual isopycnals were determined by linear interpolation of the data immediately above and below the target density. Should there be no data within a $\sigma_1 = 0.2$ interval (200 to 300 m) of the target density, then the station is rejected. The RSW layer is defined as the interval $\sigma_1 = 31.5$ to 32.1 ($\sigma_0 \approx 27.0$ to 27.6) (see section 3), and data within these density levels were averaged to give a value for the layer. In order to handle and map this large data set, objective analysis was used to diagnose the mesoscale field after removing large-scale means from the property field.

There are many papers dealing in the theory and practical use of objective analysis in oceanography [e.g., *Davis*, 1985; *Freeland and Gould*, 1976; *Chereskin and Trunnel*, 1996], and the reader is referred to these papers for a more detailed description. The analysis we used is based on the technique of *Bretherton et al.* [1976], where the central assumption is that the mapped field is one realization from a homogeneous statistical ensemble of zero mean and known covariance. In actuality, the determination of the covariance is a difficult task since it requires a great amount of data with both temporal and spatial clarity. Therefore it is common to estimate the covariance as a function, for example, to assume that the statistics of the field are Gaussian [*Davis*, 1985]. In this case one need subjectively estimate the scale of the signal, e.g., its correlation length scale, so that with an associated noise the covariance can be calculated. Here we take the correlation length scale to be isotropic and constant throughout the do-

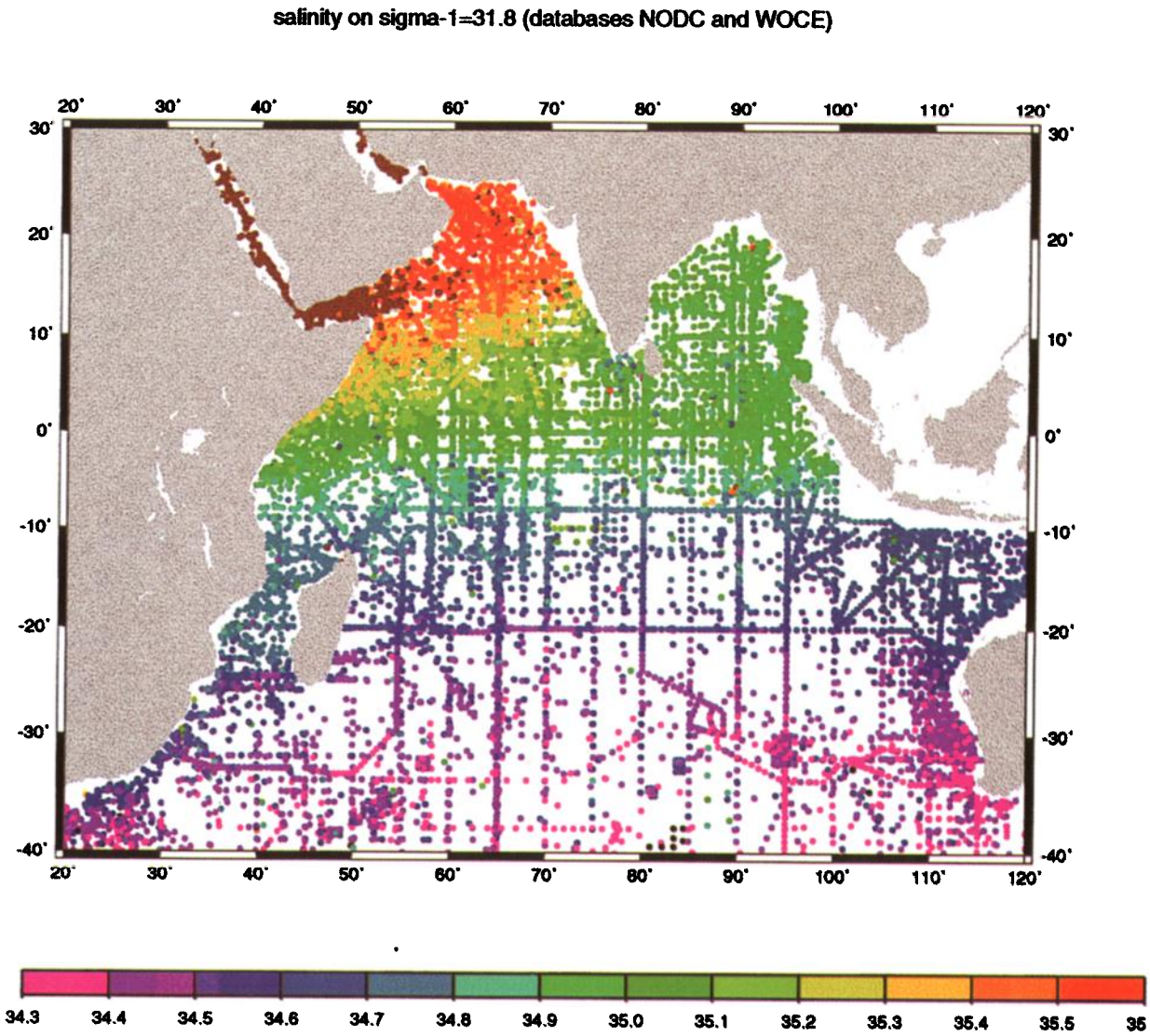

Plate 1. Positions of stations from the combined NODC and WOCE database on $\sigma_1 = 31.8$ ($\sigma_0 = 27.3$), that is, the core density of the RSW layer. Colors represent varying salinity as shown on the scale. Salinities >35.6 are shaded in dark red.

main of the data set. Although this is a fair assumption in the mid-ocean, one may expect that close to boundaries and at the equator the assumption is not ideal. In estimating the noise, no account is made for instrumental error or the poorer quality of measurements collected before the 1970s [*Mantyla and Reid,* 1995].

The large-scale mean must be removed from the observations prior to the objective analysis. Using a nonsimultaneous data set, as we have here, makes it easier to distinguish the difference between the mean and mesoscale field, as the two have different spatial scales, at least away from the boundary [*Le Traon,* 1990]. However, there are spatial trends in the data set: for example, the broad scale freshening of the RSW layer from northwest to southeast that makes it inappropriate to remove a constant mean throughout. In addition, the data set is large and cannot be inverted, i.e., objectively analyzed, as a single matrix. As a result, we choose to use the 200 nearest data points for each mapped grid point, over which to estimate a local mean (which is weighted using the Guassian model for the statistical correlation), remove it, and perform the objective analysis. The objective analysis routine used here was written by G. Johnson of the University of Washington. The data were objectively mapped to a 1° × 1° grid, and the analysis was performed in equal-area space, using an azimuthal equal-area projection.

3. Intermediate Water Mass Characteristics

The high-quality WHP temperature and salinity measurements enable a detailed diagnosis of the characteristics and density domain influenced by RSW on which

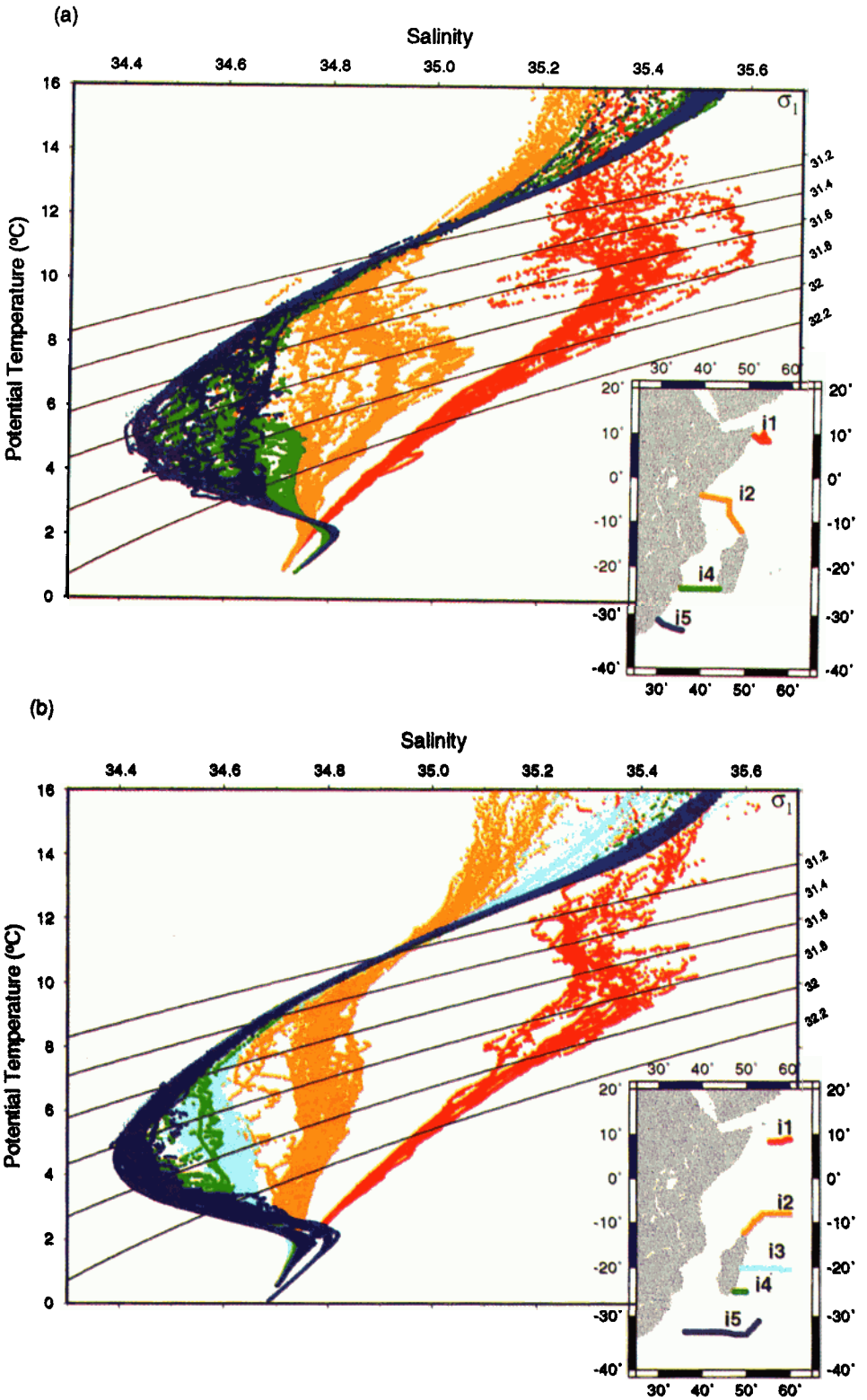

Plate 2. Temperature–salinity characteristics of intermediate waters from WOCE Indian Ocean lines I1, I2, I3, I4, and I5W. (a) Selected stations close to the western boundary and (b) selected stations farther to the east; see the insets for station positions. Red represents stations from section I1, yellow indicates data from I2, light blue indicates data from I3, green represents section I4 and blue represents stations from I5W. Contours are lines of constant potential density referenced to 1000 dbar.

to base the objective analysis. Plate 2a shows a potential temperature versus salinity ($\theta - S$) diagram of portions of zonal WOCE lines I1, I2, I4, and I5W at the western boundary. The portions of I2 and I4 enclose the Mozambique Channel at the northern and southern ends, respectively. All the sections show salty waters at intermediate depth on some stations, which are characteristic of RSW influence. The $\theta - S$ relationship of data from I4 and I5W also shows the characteristic knee of low-salinity AAIW, which *Wyrtki* [1971] found to obscure the RSW salinity maximum south of 23°S.

Plate 2a illustrates the wide density range over which the mid-depth salinity maximum due to RSW may occur. We found, as did *Warren et al.* [1966] and *Gründlingh* [1985], that the actual depth of the salinity maximum varies considerably from station to station within a single survey. This effect is even more significant when considering nonsynoptic data. As a result, one cannot follow a consistent layer by tracking the on-station salinity maximums alone. Rather, it seems more appropriate to choose a density interval over which the RSW influence is found and to use the average salinity in this layer to represent its presence. This approach has an additional advantage in that we can track the RSW beyond that latitude (23°S) at which the salinity maximum disappears owing to mixing with low-salinity AAIW [*Wyrtki*, 1971].

The spreading of RSW is seen to be predominantly isopycnic over a distance of several thousand kilometers to the south (Plate 2a), although there is evidence of some downward diapycnal migration of the salinity maximum between sections I1 and I2 as it crosses the equator. As a result, the density layer for our analysis needs to be chosen with care, so that it may best represent the density interval of RSW influence throughout the entire Indian Ocean. In the Arabian Sea the top of the RSW layer is more difficult to distinguish since there are no high-gradient thermocline waters separating the salinity maximum at mid-depth from high-salinity Persian Gulf and near-surface waters (e.g., Plate 2a, I1 data). South of the equator, the $\theta - S$ slope of the thermocline waters is very sharp and would act to significantly contaminate an averaged salinity should the upper density of the layer be chosen too shallow (e.g., Plate 2a, I5 data). Using maps of salinity on 10 isopycnic layers from $\sigma_1 = 31.2$ to 32.2 ($\sigma_0 \approx 26.7$ to 27.7), the best density interval was chosen by considering those layers which showed salinity extrema to manifest in the Gulf of Aden and at the southern edge of our Indian Ocean domain along 40°S. The resultant density interval chosen for the RSW layer is $\sigma_1 = 31.5$ to 32.1 ($\sigma_0 \approx 27.0$ to 27.6) and corresponds to a layer thickness of ~600 dbar. For comparison, *Gründlingh* [1985] estimated the density interval of RSW influence to be $\sigma_0 = 27.0$ to 27.7 at latitudes between 25° and 30°S, and *Warren et al.* [1966] estimated $\sigma_0 = 27.0$ to 27.6 in the Somali Basin, between 12°N and the equator. Hereafter we refer to this density interval, $\sigma_1 = 31.5$ to 32.1, as the RSW layer.

The WOCE data can also give a preliminary indication of the spatial variability of RSW influence. Plate 2b, shows the $\theta - S$ relationship for portions of the same sections shown in Plate 2a, but farther east and outside the Mozambique Channel (see inlaid map). There is a marked contrast between Plates 2a and 2b; the salinity, and therefore RSW influence, is much reduced away from the western boundary. South of the equator, there is evidence of RSW at only a couple of stations along I4 this far east, leaving a strong suggestion that the primary southward path for RSW may be through the Mozambique Channel. However, the presence of RSW may be intermittent, and its mean path may not be well represented by one-time data. For instance, while there is almost no influence of RSW on section I5W east of 35°E (Plate 1b), *Gründlingh* [1985] encountered lenses of RSW approximately 50 km across and up to 800 dbar thick as far east as 40°E, over the Mozambique Ridge, during three surveys in 1981.

4. A Simple Mixing Model

In addition to mapping the average properties of the RSW layer throughout the Indian Ocean, we wish to quantify the amount of RSW present in the layer in terms of a simple water mass mixing model. The concept for this model is a linear mixing of RSW and AAIW within the density interval. However, there are other potential fluxes of salt into the layer, and these are considered below, to test the robustness of this model.

The $\theta - S$ relationship of Plate 2 indicates that there exist just two water masses at intermediate depths in the Indian Ocean: RSW and AAIW [*Toole and Warren*, 1993; *Fine*, 1993]. However, there is a third intermediate water mass which occurs in the Indian Ocean between 5° and 20°S and flows from the Indonesian Seas in the east. *Rochford* [1966] refers to it as Banda Intermediate Water (BIW) and identifies it as a salinity minimum of 34.6 on $\sigma_0 = 27.4$, at about 1000 m depth. Approximately 1.5 Sv [from *Molcard et. al*, 1996, Figure 11b] of BIW is estimated to flow into the Indian Ocean through the Timor Passage between depths of 800 and 1200 m. Another potential source of salt to our chosen density layer results from diapycnic fluxes, both diffusive and advective. The magnitude of these diapycnic fluxes can be inferred by estimating the convergence of salt into the layer owing to RSW, BIW, and the horizontal ocean circulation, using the equations for conservation of mass and salt,

$$\rho T_{RSW} + \rho T_{BIW} + \rho T_{32} + \rho T_{dia} = 0 \qquad (1)$$

$$\rho T_{RSW} S_{RSW} + \rho T_{BIW} S_{BIW} + \rho T_{32} S_{32} + \rho T'_{32} S'_{32} + \rho T_{dia} S_{dia} + d = 0, \qquad (2)$$

Table 1. Components of the Indian Ocean Salt Budget for the Red Sea Water Layer

Component	Mass Flux, Sv	Salinity Convergence, Sv psu
Red Sea Water	0.9	2.74±0.19
Banda Intermediate Water	1.50	0.03±0.3
Horizontal gyre	0	-2.83

The Red Sea Water Layer is defined as the density interval $\sigma_1 = 31.5$ to 32.1.

where T is volume transport, ρ is density, S is mean salinity, d is a diffusive salt flux, and $T'_{32}S'_{32}$ is the horizontal gyre export of salt at the southern extent of the Indian Ocean, taken as latitude 32°S. To solve for the diapycnic salt flux F (net advective plus diffusive) we multiply equation (1) by S_{32} and subtract it from equation (2) to get

$$F = -[T_{RSW}(S_{RSW} - S_{32}) + T_{BIW}(S_{BIW} - S_{32}) + T'_{32}S'_{32}]. \quad (3)$$

For the RSW component the estimate of transport and salinity flowing into our density interval is discussed in detail below, but for now, we note that they are 0.9 Sv and 37.5, respectively. Previously we noted that for BIW these values are 1.5 Sv and 34.60. For an estimate of the gyre transport of salt at 32°S we use the circulation scheme diagnosed by *Robbins and Toole* [1997], who implemented both mass and silicate constraints on a hydrographic section at 32°S to obtain heat and salt budgets for the Indian Ocean. Their gyre exchange of salt within the density interval $\sigma_0 = 27.0$ to 27.6 (i.e., our RSW layer) is $T'_{32}S'_{32} = -2.83$ Sv psu, which represents an export of salt from the Indian Ocean via the Agulhas Current at the western boundary (P. E. Robbins, personal communication, 1999). We cannot be certain of the salinity at which RSW and BIW leave the Indian Ocean, but assuming that both leave via the Agulhas Current, then $S_{32} = 34.57 \pm 0.20$, allowing for large error. Table 1 summarizes the transports and salt fluxes due to each of these components.

It is clear from equation (3) and Table 1 that the residual of the salt flux components F is small, although it is unresolved. This implies that the diapycnic convergence of salt onto the RSW layer, resulting from both advective and diffusive processes, is negligible when compared to the salt input from the Red Sea. Furthermore, the salt input from the Indonesian Seas (BIW) is unresolvable from zero. Therefore we can conclude that the salt budget for the RSW layer is dominated by an influx of salt from the Red Sea and an export of salt at the southern boundary, the latter of which results from the influence of northward flowing AAIW in the interior. Thus, a simple two-end-member mixing model appears to be robust. Next we discuss and define the source water properties for each of these end-members.

The volume overflow of pure RSW through the Bab el Mandeb strait varies greatly with the monsoon seasons, almost shutting down during the summer monsoon. The strait exchange is a minimum of 0.05 Sv during July to mid-September and a maximum in February of 0.7 Sv [*Murray and Johns,* 1997]. This salty overflow water sinks into the Gulf of Aden as a gravity current, and its entrainment and mixing characteristics vary, depending on its volume flux and path. As a result, the product waters which begin to spread isopycnically (and therefore represent the end-member in our mixing model) are not well defined. There may be three or four discrete RSW layers present in the western Gulf at any time [*Bower et al.,* 1999]. Using a combination of hydrographic data and a mixing model, *Bower et al.* [1999] estimate that for the winter case (maximum outflow), the overflow reaches neutral bouyancy within just 40 km of the strait. The resultant equilibrated layer is diluted 2.5 times and has a salinity of 37.50, temperature of 18.1°C and density of $\sigma_0 = 27.2$. In the summer, when the outflow is only 0.05 Sv, *Bower et al.* [1999] find that the dilution is six-fold and the product waters are 2°C cooler. In addition to this variability, some of the overflow waters flow down a gentler and narrower channel from the strait, a path that *Bower et al.* [1999] refer to as the northern channel. This product water is less mixed and therefore is deeper ($\sigma_0 = 27.52$) and saltier (38.6) than the product waters from the main channel. While acknowledging the obvious difficulties in defining product waters precisely because of the variability discussed here, we note that the largest volume of waters are formed during winter, and choose to use these dominant winter product waters as our RSW source. However, for a flux estimate of these waters we take the annual mean volume transport of 0.37 Sv from *Murray and Johns* [1997], resulting in a flux of ~0.9 Sv (with 2.5-fold dilution) of dominant product waters of salinity 37.50.

The source of AAIW for the Indian Ocean is difficult to pinpoint. The main sites of formation are at the polar front in the western South Atlantic [*Piola and Gordon,* 1989] and to the north of the subantarctic front in the Southeast Pacific [*McCartney,* 1982]. These waters are advected eastward within the Antarctic Circumpolar Current (ACC). Maps of dynamic topography from *Wyrtki* [1971] plus the transport of the South Indian Ocean Current [*Stramma,* 1992], the pattern of wind

stress curl, and the location of most recently ventilated AAIW [*Fine*, 1993] are all consistent with equatorward flow of AAIW at about 60°E into the Indian Ocean. It may be that the shallow topography in the central south Indian Ocean limits the eastward extent of the wind-driven anticyclonic subtropical gyre to this longitude, allowing the penetration of AAIW here [*Fine*, 1993]. Hence the $\theta - S$ properties of intermediate waters found between 55° and 65°E and close to 40°S (the southward extent of our data domain) are chosen to represent the "source" of AAIW in the Indian Ocean. The salinity minimum here, averaged over the RSW layer density interval, is 34.43.

Finally, we define a percent RSW at salinity S from the two source water salinities $S_{RSW} = 37.50$ and $S_{AAIW} = 34.43$ as

$$\%RSW = \frac{100(S - 34.43)}{(37.50 - 34.43)}. \quad (4)$$

5. Mapped Properties of the Red Sea Water Layer

The results in this section are presented in four parts: first, an assessment of the semi-annual variability of the property fields; second, a discussion of the mean salinity, oxygen, and %RSW distributions; third, an investigation of the RSW signature in the vertical, as it spreads along the western boundary of the Indian Ocean; and finally, a look at the thickness of the RSW layer and its layer potential vorticity. Initially, we start with a reminder of the limitations of this analysis and what that implies for our interpretation of the results.

The data coverage was shown in Plate 1, where each CTD or bottle station is given a colored dot. The coverage is comprehensive in the northern Indian Ocean, particularly in the Arabian Sea. At the western and eastern boundaries, coverage is also good. Toward the center of the southern Indian Ocean, data become more sparse. To a large extent, the scales of variability we are able to map here are dictated by data coverage. For instance, although it is known that RSW often appears in filaments or lenses [*Gründlingh*, 1985; *Shapiro et al.*, 1994; *Beal and Bryden*, 1999] with scales of the order of 100 km across, an ocean-wide objective analysis cannot resolve these features because it is limited by data spacing, which is considerably larger than this feature scale on the whole. In addition, such features are likely nonstationary (although RSW has been measured repeatedly over the continental slope in the Agulhas Current at 32°S) and as such may not be resolved by a nonsynoptic data set spanning more than fifty years. Therefore this work does not address the patchiness of RSW influence, but rather it highlights the time-integrated pattern of the mean circulation of the water mass over the last half century. A correlation length scale of 500 km was chosen for the objective analysis, reflecting both the data coverage considerations discussed above and the expected flow scales, and to best represent the property fields and reduce mapping errors.

Tziperman [1988] has shown that a time-averaged field can be well estimated from averaged hydrographic data despite the fact that the data do not actually represent a true time average. In essence, the difference between the true time average and the one estimated from hydrographic data (as it is here) is due to the transport of water properties by eddies. The order of magnitude of these eddy fluxes is generally small when compared to the horizontal advection by the mean circulation but is of the same order as the eddy diffusion terms in the tracer equation. As a result, *Tziperman* [1988] found that while the differences in the property field for the two estimates are relatively small, the differences in estimated mixing coefficients may be the order of magnitude of the mixing coefficients. Therefore mixing coefficients calculated from climatological hydrographic data may not represent the eddy fluxes they parameterize. In addition, hydrographic data have revealed [*Gründlingh*, 1985; *Shapiro and Meschanov*, 1991] that while in some instances there is a gradual transition between RSW and AAIW, in many cases the two water masses are separated by well-defined interfaces: RSW can occur in isolated high-salinity patches or lenses. The nature of the diffusive fluxes in each of these cases would seem to be very different. As a result, we have not attempted to diagnose our results in terms of diffusive fluxes through mixing coefficients, which will likely be misleading, but instead in terms of property distributions and estimated RSW content.

5.1. Semiannual Variability

Gamsakhurdiya et al. [1991] found variability in the distribution of RSW in the Arabian Sea and attributed it almost entirely to the monsoonal changes in the Arabian Sea gyre and not to the fluctuations in transport through the Bab el Mandeb strait, which they showed to be very quickly damped beyond the Gulf of Aden. In winter they noted large southward transport of RSW, while in summer, eastward transport intensified. *Düing and Schwill* [1967] state that seasonal variations occur apparently only in the northern part of the basin and at its margins. In the Somali Basin, *Quadfasel and Schott* [1982] found evidence of seasonal spreading of RSW along the western margin and across the equator during the northeast monsoon. Changes in salinity over time were strong close to the Somali coast, but farther offshore the north-south gradient of salinity was relatively stable. They proposed that this variability is linked to Rossby Waves, which approach the western boundary between the northeast and southwest monsoons, caused by the reversing winds. On reflection at the boundary short waves are trapped, resulting in assymetrical, subthermocline transports which may be the mechanism for the Somali Undercurrent variability [*Visbeck and Schott*, 1992]. We have found no reports of

seasonality in the flow of RSW elsewhere in the Indian Ocean.

In the Arabian Sea the monsoon seasons run approximately June to September, the southwest monsoon, and November to February, the northeast monsoon. However, outside the Arabian Sea one may expect a seasonal signal in the spreading of RSW, if it exists, to become lagged or distorted. Despite this we use salinity data averaged over each monsoon season, as defined by the months given above, and calculate salinity anomalies between these periods throughout the Indian Ocean to investigate any seasonality in the spreading of RSW. We chose this method for three reasons. First, as we have seen above, seasonal variability at intermediate depths has only been reported in the Arabian Sea. Second, any seasonal signal will be a maximum in the Arabian Sea, owing to the intense forcing of the monsoon cycle and the strength of the salinity maximum. Finally, the data coverage in the Arabian Sea is excellent (Plate 1), and thus, if it is possible to determine a seasonal signal unambiguously above the noise caused by the spatial variability of data coverage, it will be here.

Salinity maps from winter (November to February inclusive) and summer monsoons (June to September inclusive) are shown in Plates 3a and b, respectively. Note that salinities of 35.8 and greater are shown in dark red; elsewhere the shading changes for every 0.1 salinity increment. Plate 3c shows the difference between Plates 3a and b, weighted by the inverse of the mapping errors, e.g. $(S_{win} - S_{sum})/E_{win+sum}$. Therefore, in regions where the mapping errors are high because of poor data coverage the salinity anomalies are reduced in magnitude. In other words, the signal that is left in Plate 3c, should be associated with regions of high-salinity variability which are not a result of changes in data coverage between the monsoons. It is conceivable that large anomalies in regions of high mapping errors may still be associated with real salinity variability, however they are ambiguous and, as such, are given a small weighting. Thus, Plate 3c highlights only those areas where there is a combination of a large salinity anomaly and small mapping errors. Red through orange patches indicate positive anomalies, blue indicate negative anomalies, and green shades indicate insignificant values.

Comparing Plates 3a and b, the salinity fields for winter and summer monsoons, the most striking difference appears along the Somali coast between 12° and 5°N. During the winter monsoon there are high salinities spreading to the south in a narrow tongue along the Somali coast, while during the summer this feature is not present. The error-weighted anomalies are significant in this region (Plate 3c), and reflect salinity differences of up to 0.15 psu. This feature compounds the work by *Quadfasel and Schott* [1982], indicating that the spreading of RSW southward along the western boundary is a phenomenon of winter monsoon conditions. There are also high anomalies in the eastern Gulf of Aden (also corresponding to salinity differences of up to 0.15), perhaps associated with the increased outflow of RSW through the Bab el Mandeb strait during the winter monsoon. Toward the center of the Arabian Sea the anomalies are patchy, correspond to salinity differences of only 0.07, and are more difficult to link with monsoonal mechanisms. There is no clear evidence to suggest that RSW spreads preferentially to the east during summer monsoon, as found by *Gamsakhurdiya et al.* [1991]. However, a number of authors [e.g., *Shapiro and Meschanov,* 1991; *Shapiro et al.,* 1994] have found the presence of RSW to the east in the Arabian Sea to be very patchy, consisting of discrete salt lenses, rather than a continuously spreading tongue, as is the case for the southward spreading along the continental margin [*Premchand et al.,* 1986; *Quadfasel and Schott,* 1982]. As a result, the spatial pattern of RSW influence is likely to change intra-monsoonally, in addition to any monsoon variability, making the signal confusing. What is clear, however, is that variability is high throughout the Arabian Sea but is not significant in the Bay of Bengal which is also under the influence of the monsoons. This suggests, in addition to the comparatively low intermediate salinities, that there is little or no spreading of RSW into the Bay of Bengal. Farther south in the Indian Ocean there is no significant monsoon variability. Although it is possible that there are other modes of variability which we were unable to detect using this method, a forcing mechanism for such variability at intermediate depth is not known to exist outside the northern Indian Ocean.

5.2. Salinity and Oxygen Fields

Plate 4a shows the layer-averaged salinity between $\sigma_1 = 31.5$ and 32.1 ($\sigma_0 \approx 27.0$ and 27.6), i.e., of the RSW layer. Errors (as estimated from the objective analysis and thus dependent on input covariance and noise) are everywhere <0.05 psu, except at the southern boundary of the domain east of 30°E. The salinity field shows a predominantly southward spreading of RSW from the mouth of the Gulf of Aden to the southern Indian Ocean. In the Arabian Sea, there is also an eastward component of spreading, following the circulation suggested by *Gamsakhurdiya et al.* [1991], although as discussed above, the evidence that this spreading is seasonally dependent is inconclusive from this study. Away from the western boundary, the spreading pattern is also consistent with the dominance of a diffusive regime in the Arabian Sea, as concluded by *Düing and Schwill* [1967] who using a simple model, found that the stationary salinity distribution is maintained through large-scale mixing processes. At the western boundary, along the East African coast, there is a tongue of high-salinity waters spreading southward, as seen during winter monsoon (Plate 3a), and crossing the equator. Since this feature is clear in the mean field, the exchange of salty water to the south along the western boundary during winter monsoon is evidently not reciprocated by

a northward exchange of relatively fresh water during summer monsoon. In fact, Plates 3a and 4a suggest that the fresher waters enter the Arabian Sea at its southeastern margin. South of the equator, in the region of the South Equatorial Current (SEC), the isohalines become almost zonal but still have a southward slope close to the western boundary. South of 12°S the spreading of RSW is very much favored through the Mozambique Channel, as previously indicated by *Wyrtki* [1971]. In the east at these latitudes the isohalines diverge toward the Indonesian Seas, as a result of the introduction of BIW here. Emerging from the Mozambique Channel is a swath of higher salinities some 800 km wide, reaching to 37°S. Within this swath is a west-east gradient of salinity, with greater values close to the South African coast in the Agulhas Current. This suggests that high salinities outside the Western Boundary Current (WBC) may result from recirculations of intermediate waters in the diffuse region of anticyclonic shear which characterizes the offshore edge of the current. Here surface instabilities, such as meanders, plumes, and eddies are common [*Lutjeharms et al.*, 1989], although less is known of the intermediate circulation. The high salinities in the Mozambique Channel and along the African coast are associated with low errors due to good data coverage (Plate 1).

Although oxygen is not a conservative property, throughout the Indian Ocean an intermediate oxygen minimum is often associated with the presence of a salinity maximum and as such can be an indicator of RSW influence [e.g., *Warren et al.*, 1966; *Beal and Bryden*, 1999]. In fact, the mid-depth oxygen minimum originates in the northern Arabian Sea, as a result of moderate consumption in waters of initially low-oxygen concentration [*Olson et al.*, 1993]. A map of average oxygen concentration in the RSW layer is shown in Plate 4b. Along the western boundary of the Indian Ocean there are many closed contours, indicating either regional sources or sinks of oxygen, or significant temporal variability within the fifty-year dataset. In the interior the contours are generally zonal but with large north-south undulations, especially in the region of the SEC. Only south of about 15°S, where there are lower oxygens in the Mozambique Channel and the Agulhas Current, does the oxygen field closely follow the salinity field. This may reflect high oxygen concentration, associated with AAIW, spreading northward from the Southern Ocean in the interior, rather than with the southward spreading of low-oxygen waters. Along the southern edge of the mapping domain, mesoscale features stretching north-south are associated with large errors of order 0.1 ml l^{-1} due to poor data coverage (also in the salinity field), although the broad doming of relatively high oxygen from the south, peaking at 60°E (disregarding the mesoscale feature), is likely an indication of the influx of AAIW to the Indian Ocean.

In the northern Bay of Bengal, Plates 4a and b show patches of slightly higher salinity and lower oxygen. It is possible that this may suggest a relatively direct supply of RSW into the Bay of Bengal along the coast of India. The salinity data from WOCE I1E, a zonal section across the mouth of the Bay along 8.5°N, show higher intermediate salinity just east of Sri Lanka, perhaps indicating a pathway for RSW along the western boundary. However, data from WOCE I9, a meridional section along 90°E, do not show higher salinities in the north and neither does *Wyrtki* [1971]. Since the salinity gradient is very small in the Bay of Bengal, some poor quality data in the large data set used here may cause an unreal trend. On the other hand, 124 stations from various cruises recorded in the NODC archive show salinities great than 35 in the Bay of Bengal, and 71 of these were sampled after 1970, when we expect better quality data [*Mantyla and Reid*, 1995]. We conclude that the features are real, but that since they are relatively isolated and represent only weak gradients, it is perhaps unlikely that they are an indication of direct RSW leakage. The low-oxygen concentration may be due to local utilization owing to the sinking of detritus from productive surface waters.

The salinity and, to a lesser extent, oxygen fields suggest a mean southward flow of waters at intermediate depths through the Mozambique Channel. Previous hydrographic surveys in the channel have shown it to be a region of high eddy activity and there is uncertainty as to the directionality of a mean flow [*Saetre and Jorge da Silva*, 1984]. The Agulhas Current is thought to be fed mainly from recirculation within the anticyclonic sub-gyre of the Southwest Indian Ocean [*Stramma and Lutjeharms*, 1997] with only about 5 Sv being contributed from the Mozambique Channel. Our results indicate that the channel is an important source of salt, at least at intermediate depth, for the Agulhas Current and therefore is a pathway for the export of saline waters to the south.

The percentage of RSW present at each station was estimated from the mixing model described in section 4. Plate 4c shows a map of percent RSW, which follows the features of the salinity field. The RSW is very rapidly diluted in the Gulf of Aden, emerging into the Arabian Sea with just 40% concentration. In the Agulhas Current, at latitudes between 27° and 37°S, there is between 5 and 6% RSW. The mapped property fields all indicate an export of RSW from the Indian Ocean in the west, via the Agulhas Current. We can approximate the export of pure RSW via the Agulhas Current by using the mapped percent RSW together with the intermediate water mass transport of the Agulhas Current given by *Beal and Bryden* [1999]. Although this transport is taken from a one-time hydrographic section, the section has been repeated a number of times historically, plus three times during WOCE [*Beal*, 1997], and

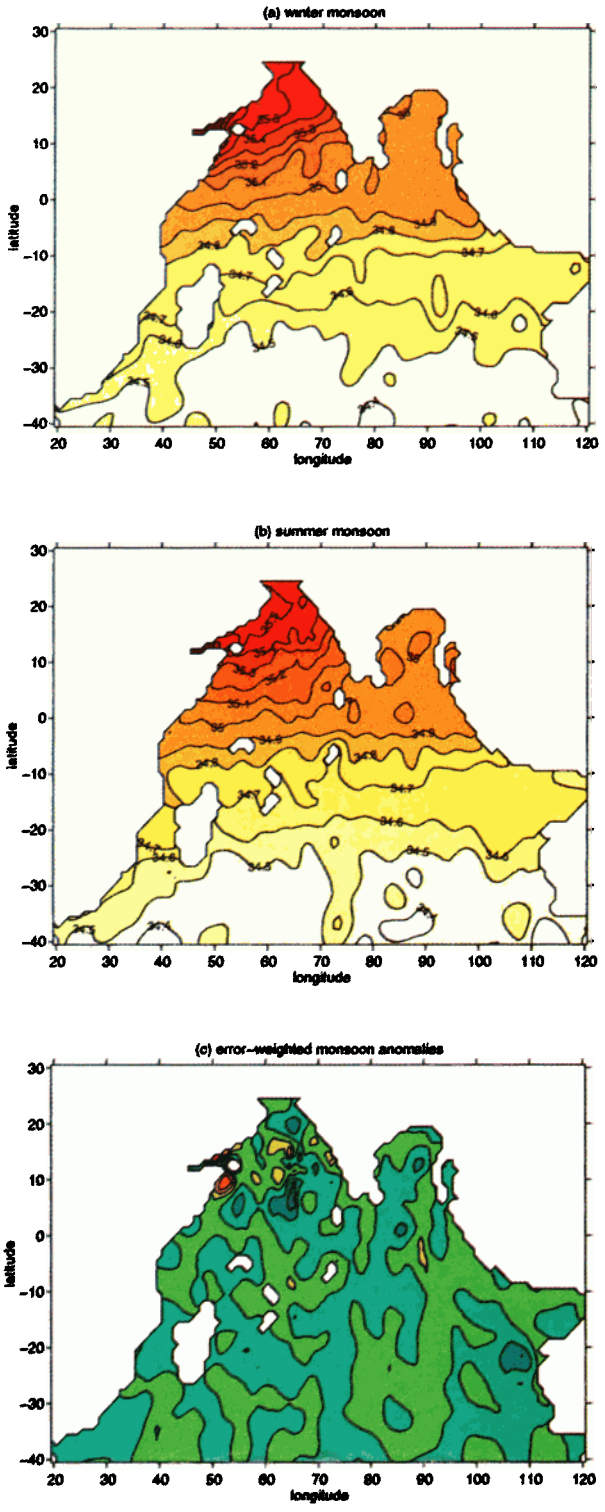

Plate 3. Maps of average salinity between $\sigma_1 = 31.5$ and 32.1 (Red Sea Water layer) for (a) winter monsoon and (b) summer monsoon. Color shades change for increments of 0.1 psu. Salinities over 35.8 are shaded in dark red. (c) The error-weighted monsoon anomaly (see text). The masking is at a resolution of 1° and defines bathymetry at 800 dbar.

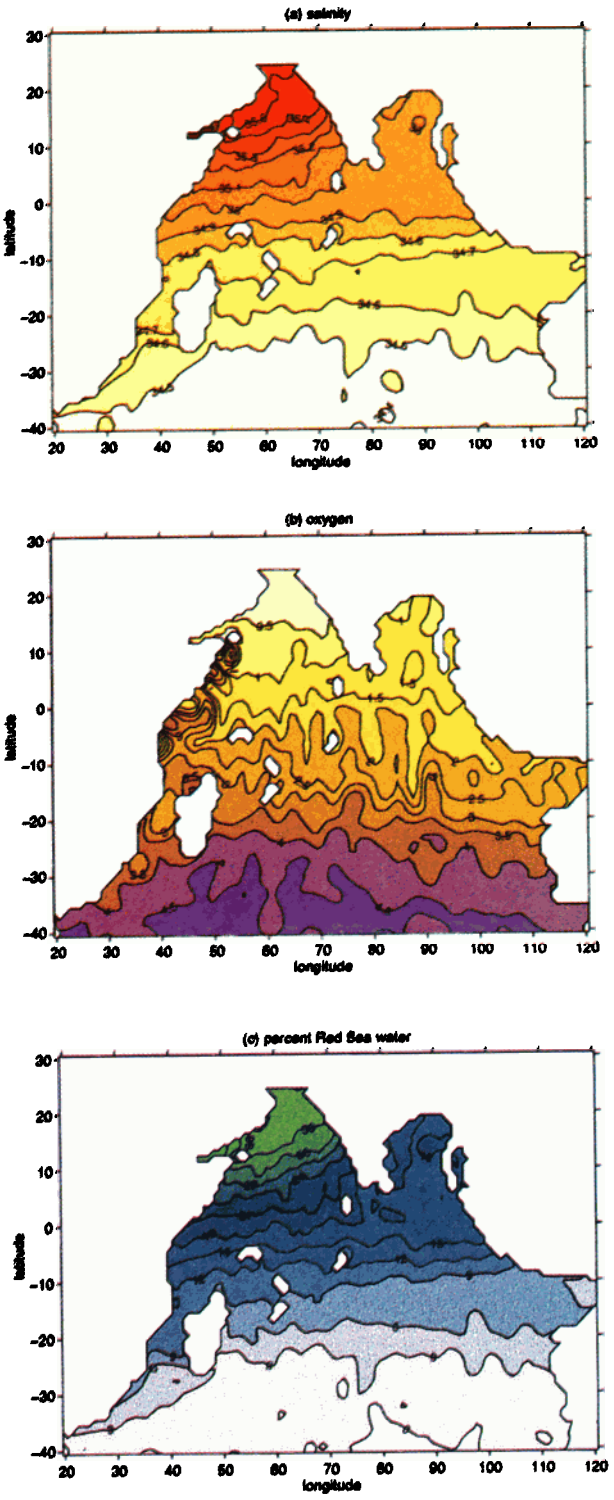

Plate 4. Maps of (a) salinity, (b) oxygen (ml l^{-1}), and (c) percent Red Sea Water, averaged over the Red Sea Water layer. Masking is as for Plate 3.

the transport has been found to be relatively invariant. Furthermore, the position and strength of the RSW filament is also consistent from section to section. Thus we assume that *Beal and Bryden's* result is representative of the mean. Recall that 100% RSW is relative to the product waters in the western end of the Gulf of Aden, which have a mean transport of about 0.9 Sv (see section 4). The volume transport of intermediate waters in the Agulhas Current, as found by *Beal and Bryden* [1999], is 19 Sv, about 5% of which is RSW (Plate 4c). This implies that there is 0.95 Sv of 100% RSW flowing southward in the Agulhas Current, or an amount equal to the influx of Red Sea product waters in the Gulf of Aden. This perhaps fortuitous result allows us two hypotheses. First, whatever RSW is mixed into the interior of the Indian Ocean it is subsequently exported at the western boundary. Second, the diapycnic convergence of salt into the RSW layer is unimportant. The circulation supports the simple isopycnic mixing model of section 4, which allows export of salt from the layer only via the Agulhas Current.

5.3. A Composite Hydrographic Section

A composite vertical section of properties along the western boundary is shown in Plate 5. Properties were averaged zonally between 27°N and 35°S and meridionally south of South Africa from 30°S to 19°S over the colored areas shown on the map inset. Note that properties in the composite section at the latitude of the Gulf of Aden (13°N) have been averaged along the length of the Gulf. Therefore the intermediate temperature and salinity increase dramatically here, as a result of the warm, salty RSW injected into the western end of the Gulf. The green contours on each plot in Plate 5 indicate the isopycnals at the top and bottom of our RSW layer (i.e., $\sigma_1 = 31.5$ and 32.1).

In the Arabian Sea, RSW and Persian Gulf Water (PGW) are of distinct origin and density. PGW has a far more northerly source and appears at depths less than 500 dbar. There is little evidence of this water mass spreading southward, perhaps owing to a vigorous mixing rate. The RSW input appears between 500 and 900 dbar and spreads southward from the mouth of the Gulf of Aden as a salinity maximum which disappears between 20° and 25°S, as shown previously by *Wyrtki* [1971]. The salinity maximum of the RSW tongue becomes denser as it spreads southward, showing that the flux of salt is not purely isopycnic, however the maxima are everywhere captured within the density interval of our RSW layer. The oxygen concentration appears to follow salinity closely in this vertical section, unlike the evidence from the mapped fields. This may be owing to the extensive smoothing that was required in order to produce the composite section. However, the mid-depth low-oxygen layer is much thicker than the high-salinity layer and evidently spreads from the far northern Arabian Sea. There is an indication that both the salt and oxygen tongues appear to flow underneath the AAIW spreading from the south. The freshwater tongue of AAIW deepens by almost 500 dbar between the Atlantic and Indian Oceans, dipping underneath the thick Indian Ocean thermocline, closely following isopycnals. Although this composite section represents an average case that does not exist at any one moment in time in the real ocean and despite the extensive smoothing required to produce a coherent signal, especially in the monsoonally variant regions, it provides a useful illustration of the persistence and thickness of the RSW tongue along the western boundary.

5.4. Layer Thickness and Potential Vorticity Fields

Potential vorticity (PV) can be a useful tracer for the large-scale circulation of water masses if dissipation and diabatic processes are insignificant [*McDowell et al.*, 1982; *Talley and McCartney*, 1982] and may illustrate why RSW spreads preferentially along the western boundary, as seen in Plates 2 and 4. In order to calculate PV the pressures of the upper and lower potential density bounds of the RSW layer ($\sigma_1 = 31.5$ and 32.1) were objectively mapped separately in the same manner as the other property fields onto a 1° grid. Following this, the depth field of the upper isopycnal was subtracted from the lower to give the RSW layer thickness. The layer potential vorticity was then evaluated from the planetary vorticity f and the layer thickness Δz using the equation

$$q = \frac{f}{\rho_0}\frac{\Delta\sigma_1}{\Delta z}, \tag{5}$$

where $\Delta\sigma_1 = 0.6$ is the density difference across the layer and $\rho_0 = 1031.8$ is the mid-layer density. Near the equator, as f approaches zero, the horizontal component of potential vorticity becomes more important than the vertical component calculated here, and hence this analysis is only useful away from the equator. Following *O'Dwyer and Williams* [1997] we take the potential vorticity at the equator to be zero.

Maps of the pressure, thickness, and PV of the RSW layer are shown in Plates 6a, b and c, respectively. The layer is centered between 800 and 900 dbar throughout the northern Indian Ocean until it crosses 10°S; thereafter it deepens toward the southwest Indian Ocean subgyre, reaching a maximum pressure of 1200 dbar, before rising rapidly west of 55°E in the region of the subtropical convergence at 40°S. In a narrow strip along the western boundary the layer remains centered at 900 dbar or less, except in a small area in the southern Mozambique Channel.

As far as layer PV is concerned, there appears to be three regimes of q; the first is north of approximately 10°S, the second is between 10 and 23°S and the third

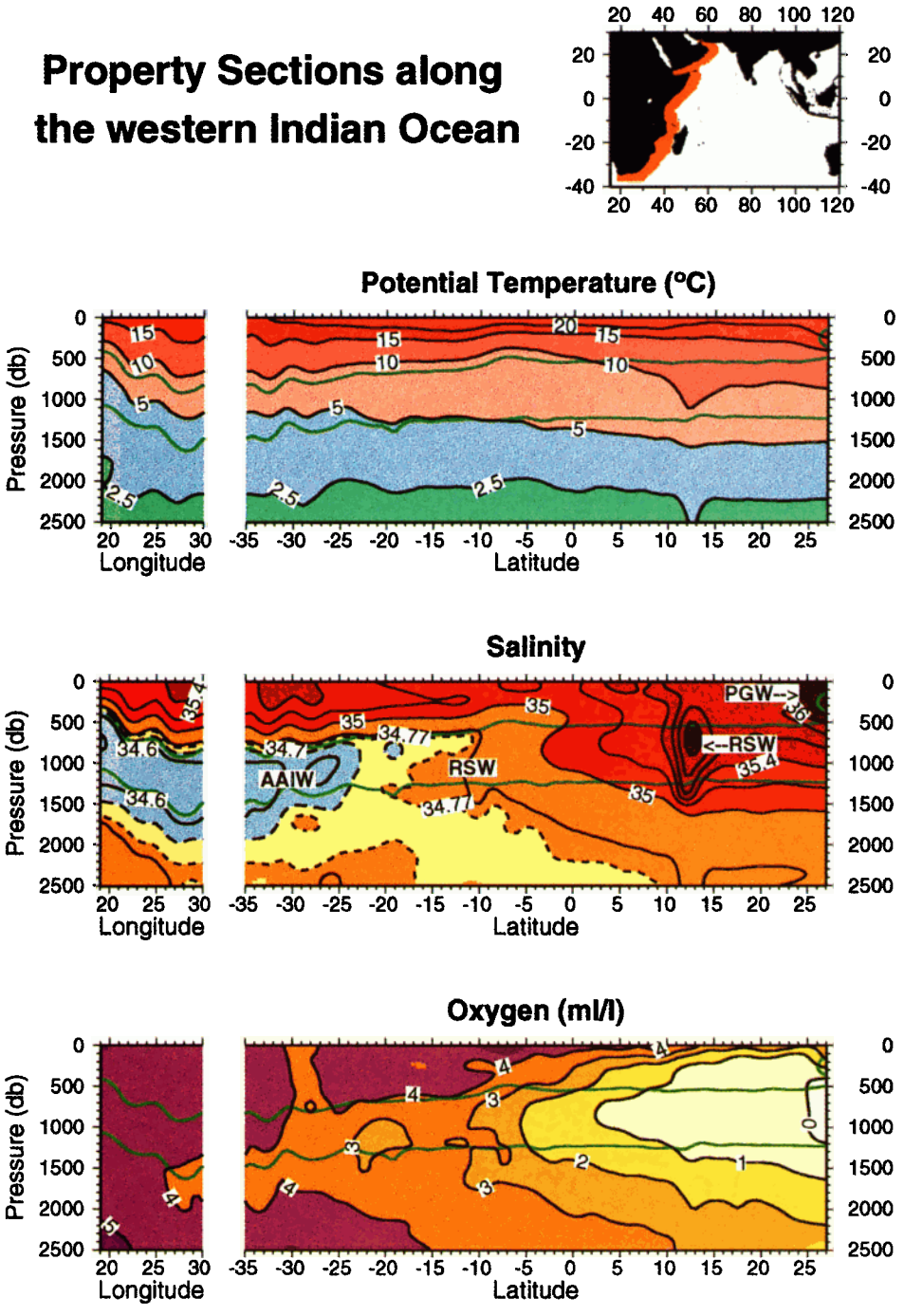

Plate 5. Vertical sections of temperature, salinity, and oxygen (ml l^{-1}) along the western boundary of the Indian Ocean.

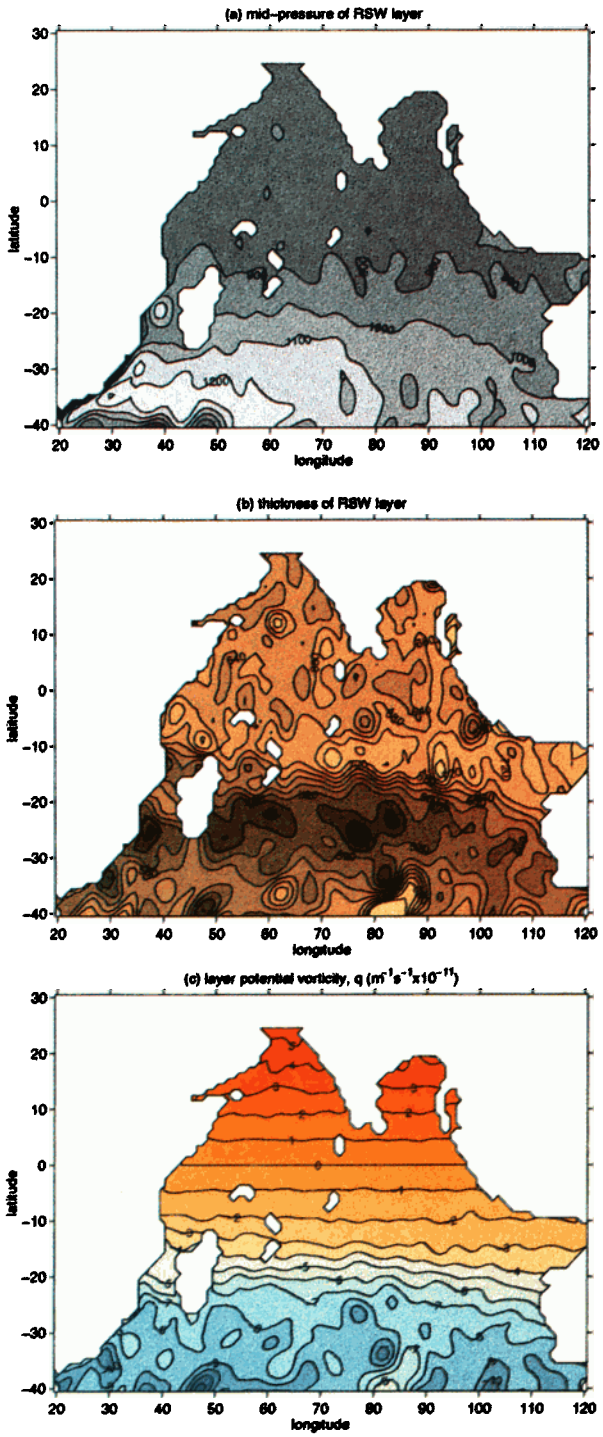

Plate 6. Maps of (a) the mid-pressure (dbar), (b) layer thickness (dbar), and (c) layer potential vorticity ($m^{-1}s^{-1} \times 10^{-11}$) for the Red Sea Water layer. Layer potential vorticity is calculated from layer thickness (converted to m) and planetary vorticity (see equation (1)).

is south of 23°S. North of 10°S, the q contours tend to follow lines of latitude since the layer thickness here is relatively unchanging (Plate 6b), and they intersect the continents, indicating that there is no "free" meridional flow; i.e., there is no energy-conserving meridional flow because lines of constant PV must be crossed. The RSW layer has its greatest vertical thickness at about 10°S, coincident with the SEC (which occurs at the much shallower depth of 200 m) and with the influx and spreading of BIW into the layer. Between 10° and 23°S the meridional gradient of q is greatest, suggesting a stronger resistance to meridional flows. This pattern reflects the rapid change in layer thickness in this region, from 700 dbar in the north to less than 500 dbar farther south. In the northern Mozambique Channel, however, q is almost invariant, and the layer thickness gradient switches between negative and positive twice, producing an alternating pattern of increased and decreased stratification, perhaps reflecting the dominance of eddying flows in the channel. Finally, south of 23°S the zonal nature of the potential vorticity gradient almost disappears, owing to the combined effect of decreasing planetary vorticity and increasing layer depth, suggesting a relatively free meridional flow of waters.

There is not an obvious indication of a freer path for RSW along the western boundary, except perhaps in the northern Mozambique Channel and in the Agulhas Current (barely resolved). These are regions where, from the property fields shown earlier (Plate 4), the western boundary path southward seems most preferentially selected. On the whole, for RSW to spread southward there has to be a diabatic modification of q and this may occur as a result of localized mixing enhanced by steep or rough topography [*O'Dwyer and Williams,* 1997]. In fact, according to the work of *Sjöberg and Stigerbrand* [1992], the Mozambique Channel is one of the few regions in the world's oceans (among them the Indonesian Seas and the Bay of Biscay) where energy fluxes to internal tides exceed 0.1 W m^{-2}. Areas of internal wave generation are thought to be areas of intense mixing due to wave breaking and the generation of turbulence. This may explain the preferred route for RSW through the Mozambique Channel.

6. Conclusions

There is monsoonal variability of the spreading of RSW in the Arabian Sea. In particular, during the winter monsoon, there is enhanced spreading within the Gulf of Aden and southward along the Somali coast, in agreement with previous surveys [e.g., *Quadfasel and Schott,* 1982]. Within the Arabian Sea interior the RSW layer appears well mixed, perhaps partially as a result of the monsoonally reversing pressure field. There is no significant spreading of RSW directly into the Bay of Bengal, the salinity field indicating that eastward spreading of RSW occurs in the equatorial region. The tongue of RSW at the western boundary in the Arabian Sea is also evident in the mean field and continues southward, crossing the equator and spreading through the Mozambique Channel and on into the Agulhas Current. Between 10° and 15°S in the Indian Ocean interior the westward spreading of BIW and high PV gradients result in a partial squeezing of the RSW layer from 700 to 500 dbar thickness. In the Mozambique Channel,

however, the penetration of BIW is limited, and the high PV gradient appears farther to the south, allowing RSW relatively free entry into the northern channel and perhaps explaining its preferred western route. Once into the southwest Indian Ocean sub-gyre, RSW is rapidly advected along the South African coast within the Agulhas Current.

The most notable conclusions from this analysis are the following. There is implication of a relatively stationary, preferred path for waters of Red Sea origin southward along the length of the western boundary of the Indian Ocean, particularly within the Somali Undercurrent, through the Mozambique Channel, and into the Agulhas Current. Furthermore, an estimate of the RSW content of the Agulhas Current implies that of the salt injected into the intermediate layers of the Indian Ocean from the Red Sea overflow, all may eventually be exported from the ocean via the Agulhas Current. This result also suggests that the net flux of salt into this layer, owing to both advective and diffusive diapycnic processes, is negligible when compared to the salt input from the Red Sea. Both these inferences have a strong implication for the importance of RSW to the global thermohaline circulation. The extreme salt content of RSW, although much reduced by 30° to 40°S, would nevertheless be a significant source of salt (34.6) to the fresh intermediate waters of the eastern South Atlantic (34.3), and indeed, RSW has been sampled at the Agulhas Retroflection [*Gordon et. al,* 1987] and inside an Agulhas ring [*Valentine et al.,* 1993] in the South Atlantic.

Acknowledgments. The authors wish to thank all the WHP Indian Ocean PIs for making available their preliminary data sets on the World Wide Web. L.M.B. is particularly grateful to Paul Robbins of the Scripps Institution of Oceanography for many useful discussions and to Alex Orsi of Texas A & M University for challenging discussions on objective analysis. We are grateful to Greg Johnson for allowing his objective analysis software to be used throughout the wider community. Many thanks to Phil Mele and Bruce Huber for their patient technical support. This work was supported by NOAA grant NA66GP0267 and NSF grant OCE 97-29322 and represents contribution number 6005 of the Lamont-Doherty Earth Observatory. L.M.B. acknowledges support from OCE-9413174 while this manuscript was revised.

References

Beal, L. M., Observations of the velocity structure of the Agulhas Current, Ph.D. dissertation, 156 pp., University of Southampton, 1997.

Beal, L. M., and H. L. Bryden, Observations of an Agulhas Undercurrent, *Deep Sea Res., Part I, 44* 1715-1724, 1997.

Beal, L. M., and H. L. Bryden, The velocity and vorticity structure of the Agulhas Current at 32°S, *J. Geophy. Res., 104*, 5151-5176, 1999.

Bower, A. S., H. D. Hunt, and J. F. Price, Character and dynamics of the Red Sea and Persian Gulf outflows, *J. Geophys. Res.*, in press, 1999.

Bretherton, F. P., R. E. Davis, and C. B. Fandry, A technique for objective analysis and design of oceanographic experiments applied to MODE-73, *Deep Sea Res., 23*, 559-582, 1976.

Chereskin, T. K., and M. Trunnel, Correlation scales, objective mapping, and absolute geostrophic flow in the California Current,*J. Geophy. Res., 101*, 22,619-22,629, 1996.

Davis, R. E., Drifter observations of coastal surface currents during CODE: The statistical and dynamical views, *J. Geophys. Res., 90*, 4756-4772, 1985.

Düing, W., and W. D. Schwill, Ausbreitung und Vermischung des salzreichen Wassers aus dem Roten Meer und dem Persischen Golf, *Meteor Forschungsergeb. Reihe, A, 3*, 44-66, 1967.

Fedorov, K. N., and S. L. Meschanov, Structure and propagation of Red Sea waters in the Gulf of Aden, *Oceanology, 28*, 279-284, 1988.

Fine, R. A., Circulation of Antarctic Intermediate Water in the South Indian Ocean, *Deep Sea Res., Part I, 40*, 2021-2024, 1993.

Freeland, H. J., and W. J. Gould, Objective analysis of meso-scale ocean circulation features, *Deep Sea Res., 23*, 915-923, 1976.

Gamsakhurdiya, G. R., S. L. Meschanov, and G. K. Shapiro, Seasonal variations in the distribution of Red Sea waters in the northwestern Indian Ocean, *Oceanology, 31*, 32-37, 1991.

Gordon, A. L., J. R. E. Lutjeharms, and M. L. Gründlingh, Stratification and circulation at the Agulhas Retroflection,*Deep Sea Res., Part A, 34*, 565-599, 1987.

Gründlingh, M. L., Occurrence of Red Sea Water in the southwestern Indian Ocean, 1981, *J. Phys. Oceanogr., 15*, 207-212, 1985.

Le Traon, P. Y., A method for optimal analysis of fields with spatially variable mean, *J. Geophys. Res., 95*, 13,543-13,547, 1990.

Lozier, M. S., M. McCartney, and W. B. Owens, Anomalous anomalies in averaged hydrographic data, *J. Phys. Oceanogr., 24*, 2624-2638, 1994.

Lutjeharms, J. R. E., R. Catzel, and H. R. Valentine, Eddies and other boundary phenomena of the Agulhas Current,*Cont. Shelf Res., 9*, 597-616, 1989.

Mantyla, A. W., and J. Reid, On the origins of deep and bottom waters of the Indian Ocean, *J. Geophys. Res., 100*, 2417-2439, 1995.

McCartney, M. S., The subtropical recirculation of Mode Waters, *J. Mar. Res., 40*, 427-464, 1982.

McDowell, S., P. Rhines, and T. Keefer, North Atlantic potential vorticity and its relation to the general circulation, *J. Phys. Oceanogr.,12*, 1417-1436, 1982.

Molcard, R., M. Fieux, and A. G. Ilahude, The Indo-Pacific throughflow in the Timor Passage, *J. Geophy. Res., 101*, 12,411-12,420, 1996.

Murray, S. P., and W. Johns, Direct observations of seasonal exchange through the Bab el Mandab Strait, *Geophys. Res. Lett., 24*, 2557-2560, 1997.

O'Dwyer, J., and R. G. Williams, The climatological distribution of potential vorticity over the abyssal ocean, *J. Phys. Oceanogr., 27*, 2488-2506, 1997.

Olson, D. B., G. L. Hitchcock, R. A. Fine, and B. A. Warren, Maintenance of the low- oxygen layer in the central Arabian Sea, *Deep Sea Res., Part I, 40*, 673-685, 1993.

Piola, A. R., and A. L. Gordon, Intermediate water in the south western South Atlantic, *Deep Sea Res., Part A, 36*, 1-16, 1989.

Premchand, K., J. S. Sastry, and C. S. Murty, Watermass structure in the western Indian Ocean, part III; The spreading and transformation of Red Sea watermass, *Mausam, 37*, 317-324, 1986.

Quadfasel, D. R., and F. Schott, Water mass distributions at intermediate layers off the Somali coast during the onset

of the southwest monsoon, *J. Phys. Oceanogr.*, *12*, 1358-1372, 1982.

Robbins, P. E., and J. M. Toole, The dissolved silica budget as a constraint on the meridional overturning circulation in the Indian Ocean, *Deep Sea Res., Part I*, *44*, 879-906, 1997.

Rochford, D. J., Distribution of Banda intermediate water in the Indian Ocean, *Aust. J. Mar. Freshwater Res.*, *17*, 61-76, 1966.

Saetre, R., and A. Jorge da Silva, The circulation of the Mozambique Channel, *Deep Sea Res., Part A*, *31*, 485-508, 1984.

Shapiro, G. I., and S. L. Meschanov, Distribution and spreading of Red Sea Water and salt lens formation in the northwest Indian Ocean, *Deep Sea Res., Part A*, *38*, 21-34, 1991.

Shapiro, G. I., S. L. Meschanov, and A. B. Polonsky, Red Sea water lens formation in Arabian Sea, *Oceanology*, *34*, 26-31, 1994.

Sjöberg, B., and A. Stigerbrand, Computations of the geographical distribution of the energy flux to mixing processes via internal tides and the associated vertical circulation in the ocean. *Deep Sea Res., Part A*, *39*, 269-291, 1992.

Stramma, L., The South Indian Ocean Current, *J. Phys. Oceanogr.*, *22*, 421-430, 1992.

Stramma, L., and J. R. E. Lutjeharms, The flow field of the subtropical gyre of the South Indian Ocean, *J. Geophys. Res.*, *102*, 5513-5530, 1997.

Talley, L. D., and M. S. McCartney, Distribution and circulation of Labrador Sea Water, *J. Phys. Oceanogr.*, *12*, 1189-1205, 1982.

Toole, J. M., and B. A. Warren, A hydrographic section across the subtropical South Indian Ocean, *Deep Sea Res. Part I*, *40*, 1973-2019, 1993.

Tziperman, E., Calculating the time-mean oceanic general circulation and mixing coefficients from hydrographic data, *J. Phys. Oceanogr.*, *18*, 519-525, 1988.

Valentine, H. R., J. R. E. Lutjeharms, and G. B. Brundrit, The water masses and volumetry of the southern Agulhas Current region, *Deep Sea Res. Part I*, *40*, 1285-1305, 1993.

Visbeck, M., and F. Schott, Analysis of seasonal current variations in the western equatorial Indian Ocean: Direct measurements and GFDL model comparison, *J. Phys. Oceanogr.*, *22*, 1112-1128, 1992.

Warren, B. A., H. Stommel, and J. C. Swallow, Water masses and patterns of flow in the Somali Basin during the southwest monsoon of 1964, *Deep Sea Res.*, *13*, 825-860, 1966.

Wyrtki, K., *Oceanographic Atlas of the International Indian Ocean Expedition*, 531 pp., Nat. Sci. Found., Washington, D.C., 1971.

You, Y., and M. Tomczak, Thermocline circulation and ventilation in the Indian Ocean derived from water mass analysis, *Deep Sea Res., Part I*, *40*, 13-56, 1993.

L. M. Beal, Scripps Institution of Oceanography, 9500 Gilman Drive, La Jolla, CA 92093-0230. (lbeal@ucsd.edu)

A. Ffield and A. L. Gordon, Lamont-Doherty Earth Observatory of Columbia University, Palisades, NY 10964.

(Received October 21, 1998; revised September 23, 1999; accepted October 14, 1999.)